



Tunable spectral response by hydrogen irradiation of Ga(AsN) superlattice diodes


N. Balakrishnan, G. Pettinari, O. Makarovsky, M. Hopkinson, and A. Patanè

Citation: [Applied Physics Letters](#) **104**, 242110 (2014); doi: 10.1063/1.4884425


View online: <http://dx.doi.org/10.1063/1.4884425>

View Table of Contents: <http://scitation.aip.org/content/aip/journal/apl/104/24?ver=pdfcov>

Published by the [AIP Publishing](#)




Agilent's Electronic Measurement Group is becoming **Keysight Technologies**.



Engineering Education & Research Resources DVD 2014

Agilent is the key to your test and measurement needs **Order yours**

**Agilent Technologies**

Tunable spectral response by hydrogen irradiation of Ga(AsN) superlattice diodes

N. Balakrishnan,^{1,a)} G. Pettinari,² O. Makarovskiy,¹ M. Hopkinson,³ and A. Patané^{1,a)}

¹*School of Physics and Astronomy, University of Nottingham, Nottingham NG7 2RD, United Kingdom*

²*National Research Council (CNR), Institute for Photonics and Nanotechnologies (IFN-CNR), via Cineto Romano 42, 00156 Roma, Italy*

³*Department of Electronic and Electrical Engineering, University of Sheffield, S3 3JD Sheffield, United Kingdom*

(Received 1 April 2014; accepted 9 June 2014; published online 18 June 2014)

We report on the tuning of the spectral response of superlattice (SL) diodes based on dilute nitride Ga(AsN) alloys by *post-growth* hydrogenation. Hydrogen is incorporated into the superlattice where it neutralizes the electronic activity of nitrogen by forming N-H complexes. We exploit the controlled thermal dissociation of the complexes to tune the energy of the SL photocurrent absorption and electroluminescence emission; also, by annealing a submicron spot with a focused laser beam we create a preferential path for the injection of carriers, thus activating a nanoscale light emitting region. This method can be used for fabricating planar diode arrays with distinct optical active regions, all integrated onto a single substrate. © 2014 AIP Publishing LLC.

[<http://dx.doi.org/10.1063/1.4884425>]

The nitrogen-induced band gap reduction in III-V semiconductor compounds^{1,2} is a remarkable physical phenomenon in condensed matter physics and makes dilute nitride III-N-V alloys promising candidates for several applications, including nanophotonics³ and photovoltaics.⁴ Of particular interest is the combined effect of nitrogen and hydrogen atoms on the electronic properties of a III-V compound. Hydrogen atoms are highly mobile and reactive elements that bind to several atomic species. They can passivate both deep and shallow crystal defects and impurities in semiconductors;^{5,6} in particular, in III-N-Vs hydrogen tends to form dihydrogen-nitrogen complexes,⁷⁻¹⁰ which are responsible for the neutralization of the electronic activity of nitrogen and the restoration of the band gap energy to its original value in the host crystal. This phenomenon has important technological applications. Hydrogenation combined with lithography and masking of an optically active dilute nitride III-N-V alloy has been used to fabricate ordered arrays of zero-dimensional nanostructures and site-controlled single photon emitters;^{3,8} also, hydrogenation and laser writing of a III-N-V alloy provide a versatile top-down approach to a spatial profiling of the band gap energy.^{11,12} To date, the passivation of N by H and the dissociation of N-H complexes have been examined in III-N-V epilayers and quantum wells (QWs) grown just below (<100 nm) the surface, but never implemented and demonstrated in a device structure where the active region is *deep* below the surface and embedded between doped contact layers.

In this Letter, we demonstrate that the spectral response of a GaAs_{1-x}N_x/AlAs superlattice (SL) *p-i-n* diode (Figure 1(a)) can be tuned by *post-growth* hydrogen irradiation and thermal annealing. By a controlled diffusion of hydrogen and thermal dissociation of the N-H complexes, we can finely tune both the photocurrent (PC) absorption and

electroluminescence (EL) emission energy of the SL. A focused laser beam is also used to diffuse towards the SL region hydrogen atoms *post-growth* implanted in the *p*-type GaAs top contact layer of the diode. Near band-edge states created by this process provide preferential channels for the electrical injection of carriers into the SL and activates nanoscale light emitting regions. Thus, *post-growth* hydrogenation of a diode could provide an effective route to the fabrication of photonic devices and optical integrated circuits with distinct, *tailor-made* light absorbing regions, all integrated onto a single substrate.

Our *p-i-n* SL diodes were grown by Molecular Beam Epitaxy (MBE) using a N-plasma source for the GaAs_{1-x}N_x layer. The diodes were grown on *n*⁺-GaAs (100) substrates with the following order of growth layers: A 500 nm-thick *n*⁺-doped GaAs contact layer (Si-doped to $2 \times 10^{18} \text{ cm}^{-3}$), a 50 nm *n*-doped GaAs layer ($n = 2 \times 10^{17} \text{ cm}^{-3}$), a 10 nm undoped GaAs layer, an undoped 10-period GaAs_{1-x}N_x/AlAs SL (each SL unit cell consisting of a 1 nm AlAs barrier, a 1 nm GaAs layer, a 8 nm GaAs_{1-x}N_x layer—with $x = 0, 0.35\%, 0.6\%$, or 0.85% , and a 1 nm GaAs layer), a 1 nm AlAs barrier, a 10 nm undoped GaAs layer, a 50 nm *p*-doped GaAs layer (Be-doped to $2 \times 10^{17} \text{ cm}^{-3}$), and finally a 500 nm *p*⁺-doped GaAs top contact layer ($p^+ = 2 \times 10^{18} \text{ cm}^{-3}$); see Figure 1(a). The samples were grown at 590 °C except for the SL region, which was grown at 500 °C. The nitrogen content in the GaAs_{1-x}N_x layers was determined by x-ray diffraction analysis. The *p-i-n* structures were processed using conventional optical lithography into circular mesas of diameter $d = 200 \mu\text{m}$. A ring-shaped Au/Ge electrical contact was fabricated on the top surface of the mesa to permit hydrogen implantation and measurements of the current-voltage, *I-V*, characteristics, EL, and PC spectra. In this work, positive bias is defined with the top *p*-contact layer biased positively.

The processed devices were exposed to a low-energy ($E = 100 \text{ eV}$) hydrogen-ion beam generated by a Kaufman source under different impinging nominal doses (from

^{a)} Authors to whom correspondence should be addressed. Electronic addresses: ppnb3@nottingham.ac.uk and amalia.patane@nottingham.ac.uk.

$d_H = 1 \times 10^{18}$ to 5×10^{18} ions/cm²) at various temperatures ranging from $T_H = 573$ K to 613 K and times t_H from 2 to 5 h. Following preliminary studies of the effects of hydrogen on the resistivity of the *p*-type contact layer, relatively low hydrogen doses ($d_H = 1 \times 10^{18}$ ions/cm²) were chosen to minimize the H-induced neutralization of the acceptors in the top *p*-contact GaAs layer.¹³ On the other hand, as discussed below, these doses proved to be appropriate for the diffusion of hydrogen into the GaAs_{1-x}N_x/AlAs SL.

For the PC measurements, light from a 250 W quartz halogen lamp, dispersed through a 0.25 m monochromator (bandwidth of ~ 10 nm), and modulated with a mechanical chopper, was focused onto the diode ($P \sim 10^{-3}$ W/cm²). The photocurrent signal was measured using a standard lock-in amplification technique. The micro-EL (μ EL) spectra and maps were acquired using a confocal microscope equipped with a nano-focusing system (objectives 10 \times or 100 \times), a spectrometer with a 150 g/mm grating, a CCD array photodetector, and a XY linear positioning stage. At low temperature, the EL mapping was done over a small area of the diode ($< 100 \mu\text{m}^2$) using a scanning mirror above the objective and with the diode mounted inside a cold-finger optical cryostat. For the laser writing experiments, the laser beam of a frequency-doubled Nd:YVO₄ laser ($\lambda = 532$ nm) was focused to a diameter $d < 1 \mu\text{m}$ using a 100 \times objective for a time $t_a = 20$ s and power P_a in the range of 20 to 40 mW.

Figure 1(b) shows the room temperature ($T = 296$ K) PC spectrum at $V = 0$ V of a GaAs_{1-x}N_x/AlAs SL diode with $x = 0.85\%$; see top black curve in the figure. The spectrum shows a broad excitonic absorption band, X_1 , centered at ~ 1.32 eV. This is attributed to the lowest energy interband optical transition from the hole to the electron energy mini-bands of the SL. Following H-irradiation of the diode ($d_H = 1 \times 10^{18}$ ions/cm² at $T_H = 573$ K), the intensity of the X_1 -band decreases by a factor of 10 while a stronger PC absorption is observed at $h\nu > 1.4$ eV, with a feature centered at ~ 1.45 eV (see red dashed curve in the figure), close to the energy of the X_1 band in the control sample, i.e., as grown GaAs/AlAs SL; see bottom black curve in the figure. The H-induced change of the PC spectrum was observed in all our SLs. As illustrated in Figure 1(c), the peak energy of the X_1 -band in the virgin samples is well described by a Kronig-Penney model of the SL.¹⁴ Following the hydrogenation, the photocurrent spectra of all samples show very similar shape with the peak energy of the X_1 -band corresponding to that of the as grown GaAs/AlAs SL.

Our Kronig-Penney model includes the x -dependence of the band gap energy and of the electron effective mass for bulk GaAs_{1-x}N_x, which we estimate using a two-level band-anticrossing model with a N-level located at 0.23 eV above the conduction band minimum of GaAs at $T = 296$ K and an interaction parameter $V_N = 2.7$ eV.² We have instead neglected the exciton binding energy, which represents a small correction to the calculated energies, and the effect of strain on valence band and the heavy hole effective mass, which we have assumed equal to that in GaAs ($m_{hh}^* = 0.34 m_0$, where m_0 is the electron mass in vacuum).¹⁵ For the GaAs/AlAs interface, we have also used conduction and valence band offsets of $\Delta E_c = 0.96$ eV and $\Delta E_v = 0.64$ eV, respectively.¹⁶

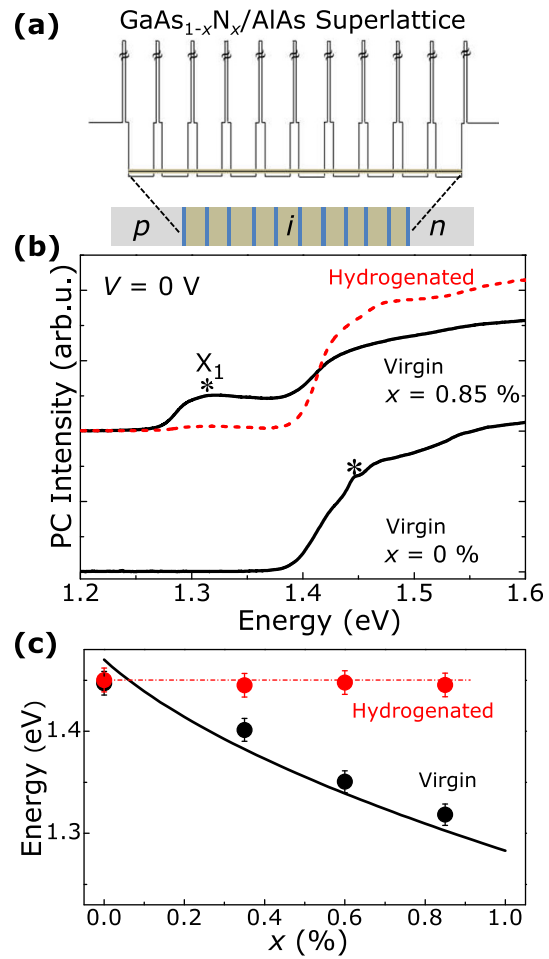


FIG. 1. (a) Conduction band profile for a *p-i-n* diode based on a GaAs_{1-x}N_x/AlAs SL with $x = 0.85\%$ at $T = 296$ K. (b) PC spectra of the virgin ($x = 0\%$ and 0.85%) and hydrogenated ($x = 0.85\%$, $d_H = 1 \times 10^{18}$ ions/cm²; $T_H = 573$ K) GaAs_{1-x}N_x/AlAs SLs at $T = 296$ K and $V = 0$ V. The excitonic PC peak, X_1 , is indicated with an asterisk. For clarity, the PC spectra are offset along the vertical axis. (c) Measured (full dots) and calculated (continuous line) values of the energy of the X_1 -band in the virgin and hydrogenated SLs versus x . The horizontal dotted line is a guide to the eye.

Our data suggest that hydrogen is incorporated well below the top GaAs *p*-type contact layer (> 500 nm) into the intrinsic SL region of the diode where it neutralizes the electronic activity of nitrogen atoms, thus restoring the pristine properties of the GaAs/AlAs SL. It is important to point out, however, that this effect is likely to be non-uniform across the 10-period SL (total length of 111 nm) where both nitrogen and nitrogen-induced crystal defects act to slow down the diffusion of hydrogen into the deepest wells of the SL. Indeed, in the hydrogenated samples, we observe a residual, weak low-energy PC absorption at the energy of the X_1 -band of the virgin sample; see, for example, the feature at ~ 1.32 eV on the PC spectrum of the hydrogenated GaAs_{1-x}N_x/AlAs SL in Figure 1(b). Post-growth hydrogenation also induces a general increase in the intensity of the EL and PL emission (by a factor of > 2), thus indicating that hydrogen has also a beneficial effect on the optical quality of the GaAs_{1-x}N_x/AlAs SL by passivating non-radiative recombination centers.

The incorporation of H into the SL and the H-induced neutralization of the nitrogen electronic activity provide us with a platform for the spectral tuning of the SL by the controlled thermal dissociation of the N-H complexes. This is

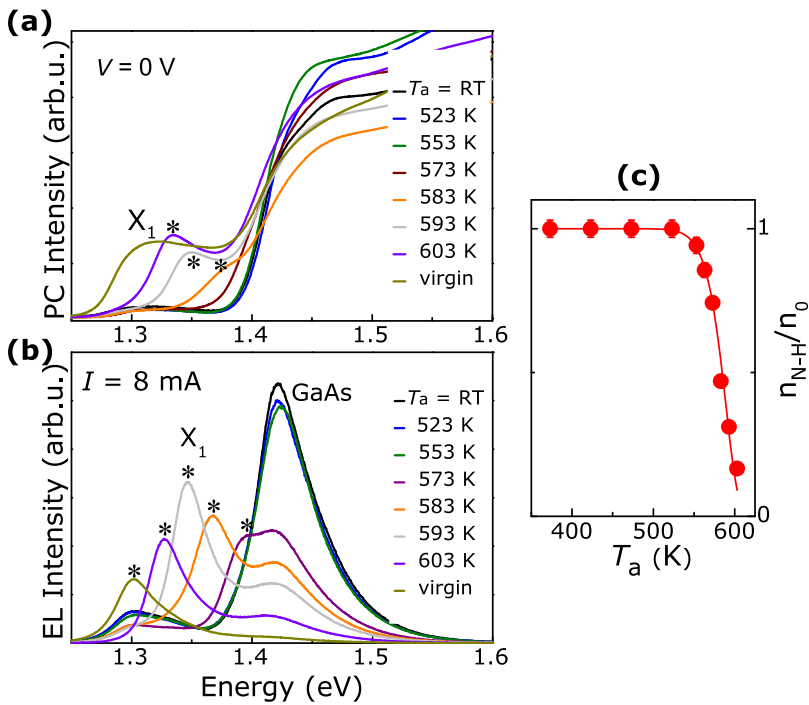


FIG. 2. PC spectra at $V = 0$ V (a) and EL spectra at $I = 8$ mA (b) for a hydrogenated ($d_H = 1 \times 10^{18}$ ions/cm²; $T_H = 573$ K) GaAs_{1-x}N_x/AlAs SL with $x = 0.85\%$ ($T = 296$ K). Spectra were measured following a 1-h thermal annealing step for increasing temperatures T_a . (c) Dependence of n_{N-H}/n_0 on T_a . The continuous line is a guide to the eye.

shown in Figure 2(a), where we plot a series of PC spectra for a hydrogenated ($d_H = 1 \times 10^{18}$ ions/cm²) GaAs_{1-x}N_x/AlAs SL with $x = 0.85\%$, each spectrum measured after 1-h step thermal annealing treatments at increasing temperatures T_a . It can be seen that increasing T_a from 523 K to 603 K induces a systematic red-shift of the X_1 -band. This is paralleled by a corresponding red-shift of the room temperature EL emission from the SL (Figure 2(b)). The energy of the emitting and absorbing regions of the SL diode can also be tuned by the annealing time t_a for a given temperature T_a . Figures 3(a) and 3(b) show the PC and EL spectra before and after each thermal annealing ($T_a = 573$ K) for a hydrogenated ($d_H = 3 \times 10^{18}$ ions/cm²) GaAs_{1-x}N_x/AlAs SL with

$x = 0.6\%$. With increasing t_a , the peak energy of the X_1 -band shifts to lower energies towards the value it has in the virgin sample. The thermal annealing promotes also a deeper penetration of hydrogen across the SL, thus leading to narrower spectral features in EL and PC (see Figure 2). Since the EL intensity is not significantly changed by the thermal annealing, the beneficial effect of hydrogen in passivating crystal defects is also preserved, thus indicating that the activation energy for breaking the N-H complex is smaller than that required to reactivate non-radiative recombination centers.

We use the peak energy position of the X_1 -band in PC spectra and the Kronig-Penney model of the SL to estimate the concentration of N-H complexes at each annealing temperature

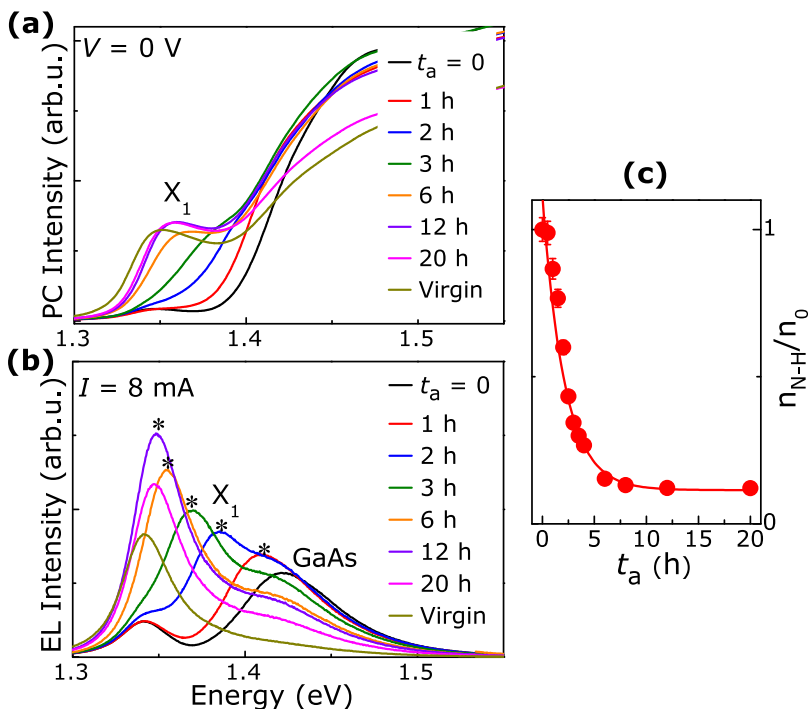


FIG. 3. PC spectra at $V = 0$ V (a) and EL spectra at $I = 8$ mA (b) for a hydrogenated ($d_H = 3 \times 10^{18}$ ions/cm²; $T_H = 573$ K) GaAs_{1-x}N_x/AlAs SL with $x = 0.6\%$ ($T = 296$ K). Spectra were measured following a thermal annealing at $T_a = 573$ K at different times t_a . (c) Dependence of n_{N-H}/n_0 on t_a . The continuous line is the fit to the data by Eq. (2) modified by a constant and with $\nu = 3$ THz.

and time. This is expressed as $n_{N-H}(T_a, t_a) = x - x_{eff}(T_a, t_a)$, where x is the N concentration in the virgin sample and $x_{eff}(T_a, t_a)$ is the concentration of N-atoms not neutralized by H in the hydrogenated sample. As shown in Figures 2(c) and 3(c), the estimated value of $n_{N-H}(T_a, t_a)$ decreases with increasing T_a (Figure 2(c)) or t_a (Figure 3(c)).

If we assume that the N-H complex dissociate irreversibly during the thermal annealing, then the rate of change of n_{N-H} can be expressed as¹⁷

$$\frac{dn_{N-H}}{dt} = -Kn_{N-H}, \quad (1)$$

where $K = \nu \exp(-\frac{E_a}{k_B T_a})$, E_a is the activation energy for the dissociation of the N-H complexes, and ν is the attempt frequency for bond breaking. Thus in steady state, $n_{N-H}(T_a, t_a)$ is given by¹⁸

$$n_{N-H}(T_a, t_a) = n_0 \exp \left[-t_a \nu \exp \left(-\frac{E_a}{k_B T_a} \right) \right], \quad (2)$$

where n_0 is the concentration of N-H bonds in the SL previous to the thermal annealing.

As shown in Figure 3(c), the measured value of $n_{N-H}(T_a, t_a)/n_0$ decreases with increasing t_a , but tends to saturate to a constant value of 0.12 at large t_a , thus suggesting the existence of a small concentration of H-related complexes that does not dissociate due to a higher activation energy. Hence, to fit the data of n_{N-H}/n_0 versus t_a , we use Eq. (2) by taking into account an additional constant term. Using for the attempt frequency ν the value of 3 THz from Ref. 19, we find that $E_a = 1.86 \pm 0.02$ eV. This value agrees very well with the activation energy for the N-H complex dissociation ($E_a = 1.89 \pm 0.02$ eV) previously obtained for $\text{GaAs}_{1-x}\text{N}_x$.¹⁹ An activation energy of 2.04 ± 0.02 eV is obtained, instead, by assuming for the attempt frequency the value (93 THz) of the N-H vibrational mode in $\text{GaAs}_{1-x}\text{N}_x$.²⁰

The *post-growth* hydrogenation and thermal annealing of a diode therefore provides an effective route for controlling the light absorption and emission of the SL. Additional versatility is enabled by the photo-stimulated diffusion of H in the *p*-type layer with a focused laser beam. A laser writing technique was used before to control the diffusion of mobile interstitial manganese (Mn_i) donor ions out of the ferromagnetic semiconductor $\text{Ga}_{1-x}\text{Mn}_x\text{As}$ towards the underlying layers of a QW heterostructure.²¹ By annealing a small spot with a focussed laser beam, it was possible to modify the local electrostatic potential in the QW plane and create a preferential path for charged carriers thus producing a nano-scale light emitting region.²¹ Here, we show that a similar result can be obtained by using atomic hydrogen, which can occupy different lattice sites and exist in different charged states in GaAs.²²

Figure 4(a) shows the μEL spectrum of the hydrogenated ($d_H = 1 \times 10^{18}$ ions/cm²) $\text{GaAs}_{1-x}\text{N}_x/\text{AlAs}$ SL with $x = 0.6\%$, measured at $V = 1.55$ V ($I = 8$ mA) and $T = 10$ K inside and outside an area exposed to a focused laser beam ($d \sim 1 \mu\text{m}$) of wavelength $\lambda = 532$ nm for a time $t_a = 20$ s and power $P_a = 40$ mW. It can be seen that the effect of the laser exposure is to increase the EL intensity of the X_1 -band by more than a factor of 10. A typical laser exposed spot can be also

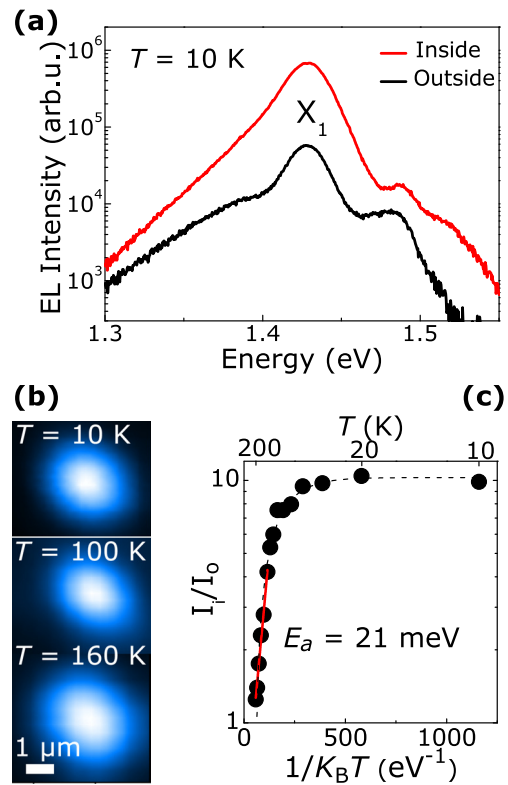


FIG. 4. (a) μEL spectra inside and outside a spot exposed to a focused laser beam ($\lambda = 532$ nm, $P_a = 40$ mW and $t_a = 20$ s) for a hydrogenated ($d_H = 1 \times 10^{18}$ ions/cm²; $T_H = 573$ K) $\text{GaAs}_{1-x}\text{N}_x/\text{AlAs}$ SL with $x = 0.6\%$ ($I = 8$ mA and $T = 10$ K). (b) μEL maps at $T = 10$ K, 100 K, and 160 K of the laser annealed spot. (c) Temperature dependence of the ratio, I_i/I_o , of the EL intensities within and outside the light emitting spot. The continuous line is a fit to the data using $I_i/I_o \sim \exp(-E_a/k_B T)$, where $E_a = 21$ meV.

resolved in the μEL map in Figure 4(b). The EL intensity distribution inside the spot has an approximately Gaussian form with a full width at half maximum that corresponds closely to the size of the laser spot diameter ($\sim 1 \mu\text{m}$). Similar μEL spectra and maps were observed in several hydrogenated samples under similar laser exposure conditions.

Since the intensity of the μPL of the laser exposed spot is not significantly changed, we suggest that the focussed laser beam acts to promote the diffusion of the hydrogen atoms thus creating a preferential path for the injection of the charged carriers into the SL region. The bright light emitting spot of the diode can be observed for temperatures up to $T \sim 200$ K (Figure 4(b)). The temperature dependence of the ratio of the EL intensities within (I_i) and outside (I_o) the laser annealed spot (Figure 4(c)) shows a thermally activated behavior described by $I_i/I_o \sim \exp(-E_a/k_B T)$, where $E_a = 21$ meV is a characteristic activation energy. Most likely, the injection of carriers into the SL takes place through states dripping from the conduction and valence band into the energy gap because of the deformation, chemical, and charge effects arising from the H interaction with the GaAs lattice.²²

Since hydrogen diffuses from the Be-doped GaAs *p*-type contact layer, the complex responsible for such states should be due to H atoms in bond center position between a Be-atom and a nearest neighbor As atom.²³ For a bond center position of hydrogen, two energy levels due to the neutral and positive charged state of H were predicted to arise at about 30 and 34 meV below the conduction band edge,

whilst two additional levels were found to be above (+5 and +30 meV) the top of the valence band.²² The binding energy of these H-induced states is close to the activation energy estimated from the temperature dependence study of the μ EL (Figure 4(c)). With increasing temperature, the emission from the diode becomes more uniform, thus suggesting the thermal ionization of these H-induced localized states and the injection of carriers into the SL through non resonant injection paths. Also, the created bright light emitting spots are visible at low temperatures ($T < 200$ K) even after many thermal cycles, thus indicating a stable modification of the diode properties by the laser-driven formation of H-induced localized states.

In conclusion, we have used a post-growth hydrogenation and thermal annealing of a diode to tune its spectral response. Our method exploits the combined effects of hydrogen and nitrogen on the electronic properties of a III–V compound: Hydrogen is diffused into a III–N–V superlattice where it neutralizes the electronic activity of nitrogen by forming N–H complexes; the controlled thermal dissociation of the complexes is then exploited to tune the photocurrent absorption and electroluminescence emission of the superlattice; alternatively, a focused laser beam is used to create preferential injection paths for the carriers thus creating a nanoscale light emitting diode. Our approach could be implemented in other materials and heterostructure devices and offers the advantage of enabling an accurate control of the spectral response of a diode using a single wafer. Also, it could enable the fabrication of planar diode arrays²⁴ with distinct light absorbing regions, all integrated onto a monolithic semiconductor structure, thus providing an alternative to re-growth techniques.

This work was supported by the University of Nottingham, the EU (under Grant Agreement No. PIER-GA-2010-272612), the Italian MIUR (under FIRB 2012 project DeLIGHTeD, prot. RBFR12RS1W), and the EPSRC. We acknowledge useful discussions with Professor Mario Capizzi and Professor Antonio Polimeni (Sapienza Università di Roma).

- ¹W. Shan, W. Walukiewicz, J. W. Ager III, E. E. Haller, J. F. Geisz, D. J. Friedman, J. M. Olson, and S. R. Kurtz, *Phys. Rev. Lett.* **82**, 1221 (1999).
- ²A. Lindsay and E. P. O'Reilly, *Phys. Rev. Lett.* **93**, 196402 (2004).
- ³S. Birindelli, M. Felici, J. S. Wildmann, A. Polimeni, M. Capizzi, A. Gerardino, S. Rubini, F. Martelli, A. Rastelli, and R. Trotta, *Nano Lett.* **14**, 1275 (2014).
- ⁴N. López, L. A. Reichertz, K. M. Yu, K. Campman, and W. Walukiewicz, *Phys. Rev. Lett.* **106**, 028701 (2011).
- ⁵J. Chevallier and M. Aucouturier, *Annu. Rev. Mater. Sci.* **18**, 219 (1988).
- ⁶C. G. Van de Walle and J. Neugebauer, *Nature* **423**, 626 (2003).
- ⁷G. Ciatto, F. Boscherini, A. Amore Bonapasta, F. Filippone, A. Polimeni, and M. Capizzi, *Phys. Rev. B* **71**, 201301 (2005).
- ⁸R. Trotta, A. Polimeni, and M. Capizzi, *Adv. Funct. Mater.* **22**, 1782 (2012) and references therein.
- ⁹A. Polimeni, G. Baldassarri Höger von Högersthal, M. Bissiri, V. Gaspari, F. Ranalli, M. Capizzi, A. Frova, A. Miriametro, M. Geddo, M. Fischer, M. Reinhardt, and A. Forchel, *Physica B* **308–310**, 850 (2001).
- ¹⁰L. Wen, F. Bekisli, M. Stavola, W. B. Fowler, R. Trotta, A. Polimeni, M. Capizzi, S. Rubini, and F. Martelli, *Phys. Rev. B* **81**, 233201 (2010).
- ¹¹N. Balakrishnan, A. Patanè, O. Makarovskiy, A. Polimeni, M. Capizzi, F. Martelli, and S. Rubini, *Appl. Phys. Lett.* **99**, 021105 (2011).
- ¹²N. Balakrishnan, G. Pettinari, O. Makarovskiy, L. Turyanska, M. W. Fay, M. De Luca, A. Polimeni, M. Capizzi, F. Martelli, S. Rubini, and A. Patanè, *Phys. Rev. B* **86**, 155307 (2012).
- ¹³G. Pettinari, N. Balakrishnan, O. Makarovskiy, R. P. Campion, A. Polimeni, M. Capizzi, and A. Patanè, *Appl. Phys. Lett.* **103**, 241105 (2013).
- ¹⁴R. De L. Kronig and W. G. Penney, *Proc. R. Soc. London, Ser. A* **130**, 499 (1931).
- ¹⁵O. Madelung, *Semiconductors: Data Handbook* 3rd ed. (Springer, New York, 2003).
- ¹⁶J. H. Davies, *The Physics of Low Dimensional Semiconductors: An Introduction* (Cambridge University press, UK, 1998).
- ¹⁷W. L. Hansen, E. E. Haller, and P. N. Luke, *IEEE Trans. Nucl. Sci.* **29**, 738 (1982).
- ¹⁸K. Bergman, M. Stavola, S. J. Pearton, and J. Lopata, *Phys. Rev. B* **37**, 2770 (1988).
- ¹⁹G. Bisognin, D. De Salvador, E. Napolitani, M. Berti, A. Polimeni, M. Capizzi, S. Rubini, F. Martelli, and A. Franciosi, *J. Appl. Crystallogr.* **41**, 366 (2008).
- ²⁰S. Kurtz, J. Webb, L. Gedvilas, D. Friedman, J. Geisz, J. Olson, R. King, D. Joslin, and N. Karam, *Appl. Phys. Lett.* **78**, 748 (2001).
- ²¹O. Makarovskiy, S. Kumar, A. Rastelli, A. Patanè, L. Eaves, A. G. Balanov, O. G. Schmidt, R. Campion, and C. T. Foxon, *Adv. Mater.* **22**, 3176 (2010).
- ²²A. Amore Bonapasta, M. Capizzi, and P. Giannozzi, *Phys. Status Solidi B* **210**, 277 (1998); *Phys. Rev. B* **59**, 4869 (1999).
- ²³P. S. Nandhra, R. C. Newman, R. Murray, B. Pajot, J. Chevallier, R. B. Beall, and J. J. Harris, *Semicond. Sci. Technol.* **3**, 356 (1988).
- ²⁴J. Herrnsdorf, E. Xie, I. Watson, N. Laurand, and M. Dawson, *J. Appl. Phys.* **115**, 084503 (2014).